

Terahertz imaging using an interferometric array

John F. Federici, Dale Gary, Brian Schulkin, Feng Huang, Hakan Altan et al.

Citation: *Appl. Phys. Lett.* **83**, 2477 (2003); doi: 10.1063/1.1610799

View online: <http://dx.doi.org/10.1063/1.1610799>

View Table of Contents: <http://apl.aip.org/resource/1/APPLAB/v83/i12>

Published by the American Institute of Physics.

Related Articles

Extension of the measurement capabilities of the quadrupole resonator
Rev. Sci. Instrum. **83**, 063902 (2012)

Enhancing photocurrent transient spectroscopy by electromagnetic modeling
Rev. Sci. Instrum. **83**, 053103 (2012)

Precise real-time polarization measurement of terahertz electromagnetic waves by a spinning electro-optic sensor
Rev. Sci. Instrum. **83**, 023104 (2012)

Smith-chart diagnostics for multi-GHz time-domain-reflectometry dielectric spectroscopy
Rev. Sci. Instrum. **83**, 025108 (2012)

Superconducting low-inductance undulatory galvanometer microwave amplifier
Appl. Phys. Lett. **100**, 063503 (2012)

Additional information on Appl. Phys. Lett.

Journal Homepage: <http://apl.aip.org/>

Journal Information: http://apl.aip.org/about/about_the_journal

Top downloads: http://apl.aip.org/features/most_downloaded

Information for Authors: <http://apl.aip.org/authors>

ADVERTISEMENT



Agilent Technologies

Agilent Education and Research Resources DVD 2012

Packed with over **100 NEW** articles, application notes, webcasts, and videos relating to Renewable Energy, Nanoscience, RF/Wireless, MIMO, Materials, Digital Signals, Photonics, and General Test & Measurement.

Click Here to
Order Your DVD



Agilent Technologies

Terahertz imaging using an interferometric array

John F. Federici,^{a)} Dale Gary, Brian Schulkin, Feng Huang, and Hakan Altan

Department of Physics, New Jersey Institute of Technology, Newark, New Jersey 07102

Robert Barat

Department of Chemical Engineering, New Jersey Institute of Technology, Newark, New Jersey 07102

David Zimdars

Picometrix Inc., Ann Arbor, Michigan 48104

(Received 19 June 2003; accepted 25 July 2003)

Most methods of imaging in the terahertz (THz) spectral region utilize either pulsed-laser sources or require the THz generation and detection sources to be phase coherent. The application of interferometric imaging to the THz range is described. Interferometric imaging offers considerable advantages in this regard due to its ability to image with only a handful of detector elements, image many sources of THz radiation at once, image incoherent as well as coherent sources, and provide spectral information as well as spatial imaging information. The THz interferometric imaging method is potentially useful for remote detection of explosives. © 2003 American Institute of Physics. [DOI: 10.1063/1.1610799]

The simplest method of terahertz (THz) imaging is to use a single transmitter and detector—i.e., line-of-sight detection. An image is obtained on a point-by-point basis by scanning the transmitter/detector pair over the sample under test and recording the THz phase and amplitude at each point. Using this method, THz images of macroscopic objects have been obtained¹ and extended to THz tomography² and synthetic phased-array techniques.³ Other THz imaging techniques are based on short-pulsed laser⁴ or cw difference frequency⁵ THz generation and detection. In the short-pulsed laser technique, the temporal profile of the THz pulse is encoded on a chirped ultrafast laser pulse. A modification of this technique has been applied to THz imaging using difference frequency mixing in nonlinear crystals. One limitation in utilizing these techniques is that coherent cw or short-pulsed laser sources are required. Moreover, the laser sources that generate and detect the THz radiation must retain a coherent phase relationship with each other. Using these methods, the imaging of an incoherent THz source is not possible.

In this letter, the design of an interferometric THz imaging array⁶ is described that does not require a particular coherent or incoherent source of THz. It is flexible enough to utilize an electronic THz source, a laser-based THz illuminating source, or incoherent ambient THz radiation that may be present. To perform imaging of THz in real time, the basic technique of radio interferometry⁷ is employed for which signals at two or more points in space (the aperture plane) are brought together with the proper delay and correlated both in phase and in quadrature to produce cosine and sine components of the brightness distribution. This technique thus measures both amplitude and phase of the incoming signals. If measured from a sufficient number of points in the aperture plane, the original brightness distribution can be synthesized (imaged) through standard Fourier inversion. The raw images after inversion can be improved through

standard image reconstruction techniques (e.g., CLEAN or MEM) to reduce ambiguities (called sidelobes) in the images.

The imaging interferometer consists of an array of individual detectors. Each detector measures the amplitude and phase of incoming THz radiation. As a wave front of THz radiation encounters the array, each pair of detectors measures one spatial Fourier component of the incoming THz radiation as determined by the separation of the detector pair, otherwise known as a base line. Each spatial Fourier component is represented by a point in the Fourier transform plane (called the $u-v$ plane). In order to determine a spatial Fourier component and consequently the direction of the incoming THz wave front, the delay in arrival time of the wave front between a pair of antennas must be measured. For a single point source, this measurement will yield an angle at which the object is located from the detector. In order to image the source, additional measurements with base lines at other spacings and orientations must be carried out.

For a given number of detectors N , there are $N(N-1)/2$ possible pair combinations. An image is generated from the spatial Fourier components of all the different pair combinations. The quality of an image depends on the coverage of the $u-v$ plane, which in turn depends on the arrangement of the detecting elements of the interferometer. The primary concern in designing the configuration of antennas is to obtain uniform and efficient coverage of the $u-v$ plane over a range determined by the required angular resolution. Efficient $u-v$ plane coverage with a small number of detectors may be achieved by rotating the array about a fixed axis. If measurements are made 20 times during the rotation of an N element array, the equivalent number of base lines will be $20N(N-1)/2$. This can either lead to improved image quality or equivalently to a reduction in the number of required detectors in the array for a given image quality.

In order to demonstrate the utility of THz interferometric imaging, THz images are simulated from a rotating and non-rotating array. For both images, the incoming THz waves are

^{a)}Electronic mail: federici@adm.njit.edu

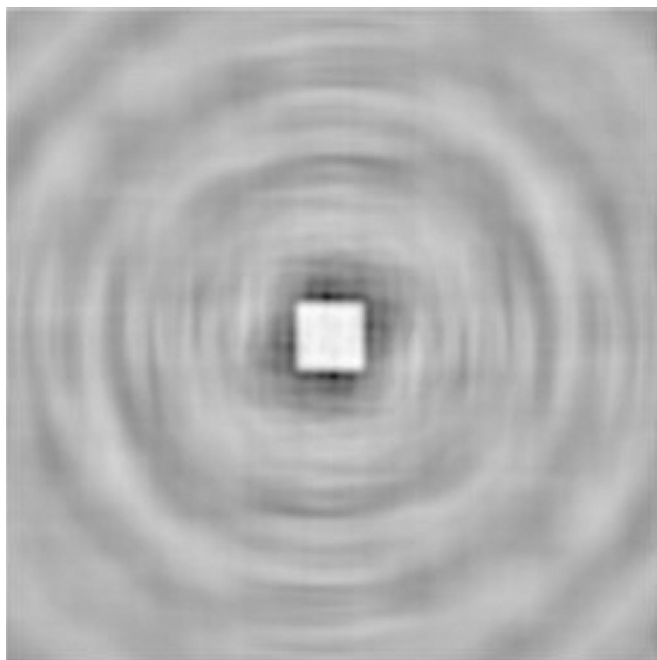


FIG. 1. Reconstructed 0.5 THz image of a 100 arc sec highly reflecting square with the 12 element rotating array with $a=0.5$ and $b=1.232\ 84$. The circular patterns in the image are sidelobe artifacts that are introduced by the imaging method. The sidelobes can be removed by image reconstruction techniques.

assumed to be plane waves. The first simulation is done for a rotating array containing 12 elements.⁶ Each detector is numbered from 1 to 12 and located alternatively on the x and y axes. The detector positions are modeled by $d=a\ b^{(n-1)}$ where d is the distance from the origin, a is a constant representing the distance of the first detector from the origin, and n is the detector number. The value b is a constant that describes the rate at which the successive detectors spiral out from the origin. Having chosen b , the constant a can be used as a multiplicative factor to normalize the overall size of the detector array for different applications. This nonredundant arrangement provides 66 Fourier components. This gives a total of 5940 Fourier components for data acquired at 1° increments for a 90° total rotation. Figure 1 is a raw image (without reconstruction) taken of a highly reflective square of angular width 100 arc sec.

The detectors of a 110 element stationary array are modeled by radial and angular positions given by $r(m)=r_0a^m$ and $\theta(m,n)=\theta_0b^{n+cm}$ where m and n are the branch and radial indices, respectively. Figure 2 shows the same object in Fig. 1 as imaged by the stationary array. For comparison, the 110 element array has 5995 Fourier components. In comparing Figs. 1 and 2, the image quality is much improved for Fig. 2 because there is more control over the dispersion of base line distances with the nonrotating array. The raw image quality of Fig. 2 rivals the quality of the (cleaned) reconstructed image (not shown) from the rotating array.

THz imaging has shown considerable promise in the detection of concealed compounds such as explosives through these materials' THz spectra. The basic concept is that the objects can be imaged at different frequencies, resulting in a cluster of images. The amplitudes of the same pixel on each image will be the spectrum of the object at that location. The ability to image these objects noninvasively at real-time

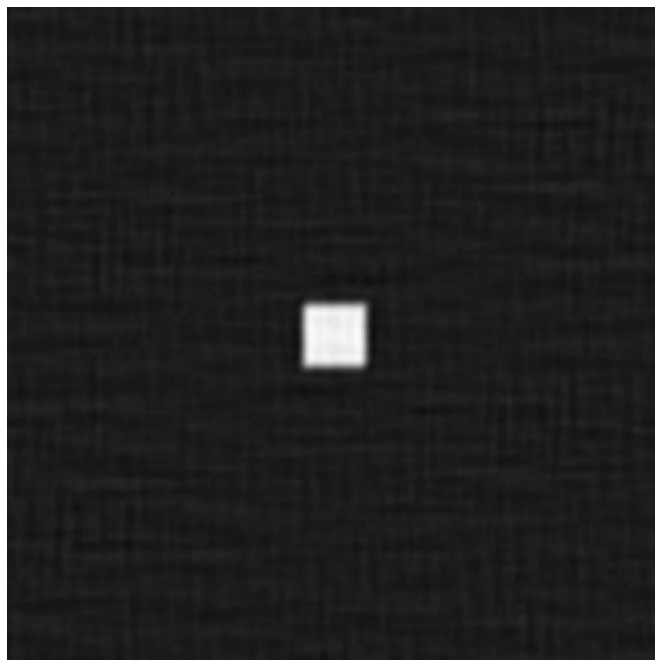


FIG. 2. Reconstructed 0.5 THz image of a 100 arc sec highly reflecting square with a fixed 110 element array. For the image, $r_0=0.5$, $a=1.2328$, $\theta_0=0.1$, $b=1.3652$, $c=0.3$, $0\leq m\leq 11$, and $0\leq n\leq 10$.

speeds has the potential to become a reliable method to remotely detect harmful objects.

As a demonstration, the addition of images is used to simulate the detection of trinitrotriazcyclohexane (RDX) and a perfect reflector, metal. RDX has a published spectrum⁸ with relatively high reflectivity at 0.75, 1.4, and 1.9 THz. Simulated images are taken at these frequencies as well as other frequencies with relative lows in the RDX reflection spectrum. Pixels in the combined image that match the RDX spectra are assigned the color red, while other pixels are assigned colors proportion to their THz frequencies (e.g., green and blue). When the THz frequency images are combined as shown in Fig. 3, the RDX appears red, while the metal appears white due to its flat reflectivity spectrum. Artificial Neural Network analysis of THz images can be used to process the composite images to distinguish materials based on their spectroscopic properties.⁹

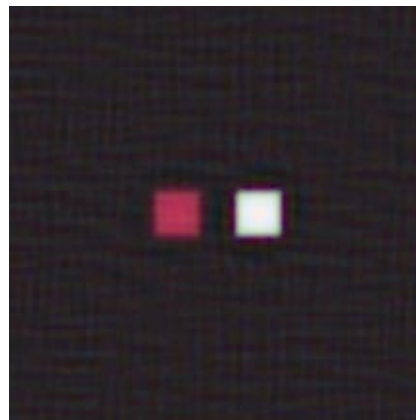


FIG. 3. (Color) Simulation of THz reflection from 2.4 cm square samples of metal (white) and RDX (red). The distance between the samples and the THz imaging array is 50 m. The false color image is a composite image of five images taken at different THz frequencies.

The angular resolution of the imaging array for a given wavelength λ is determined by the separation d between detectors: $\theta = \lambda/d$ (rad). As an example of the potential spatial resolution, a THz imaging array with maximum baseline distance of 100 cm would have an angular resolution of 62 arc sec at 1 THz. The corresponding spatial resolution at a distance of 50 m is approximately 1.5 cm.

Physical rotation of the detector array might not always be convenient to implement or desirable. Current state-of-the-art millimeter wave imaging systems depend on mechanical scanning methods for imaging with a limited number of detectors.¹⁰ However, the speed of imaging for such systems could be increased (with some tradeoffs) by increasing the number of detector elements without mechanical scanning. For example, interferometric imaging techniques could increase the effective number of pixels in real-time video displays of the millimeter wave images and possibly eliminate the need for mechanical scanning.¹¹ Nevertheless, even a state-of-the-art detector array of ~ 110 elements or larger has an insufficient pixel resolution compared to that available with a 1024×768 pixel focal plane array. Since such high density focal plane arrays are currently not feasible in the THz and gigahertz (GHz) range, interferometric imaging methods may be critical to the success of real-time imaging in the GHz and THz range.

The authors appreciate the support of the US Army through SBIR Contract No. (DAAD19-03-C-0038). Additional support through the National Science Foundation's SGER/REU Grant No. (CTS-0233582) is gratefully acknowledged. Discussions with J. M. Joseph are appreciated.

¹B. B. Hu and M. C. Nuss, Opt. Lett. **20**, 1716 (1995).

²D. M. Mittleman, S. Hunsche, L. Boivin, and M. C. Nuss, Opt. Lett. **22**, 904 (1997).

³J. O'Hara and D. Grischkowsky, Opt. Lett. **27**, 1070 (2002).

⁴Z. Jiang and X. C. Zhang, Opt. Lett. **23**, 1114 (1998).

⁵A. Nahata, J. T. Yardley, and T. F. Heinz, Appl. Phys. Lett. **81**, 963 (2002).

⁶J. F. Federici, D. Gary, B. Schulkin, F. Huang, H. Altan, R. Barat, and D. Zimdars, *International Symposium on Spectral Sensing Research*, Santa Barbara, CA, 2003.

⁷A. R. Thompson, J. M. Moran, and G. W. Swenson, *Interferometry and Synthesis in Radio Astronomy*, 2nd ed. (Wiley Interscience, New York, 2001).

⁸M. C. Kemp, P. F. Taday, B. E. Cole, J. A. Cluff, A. J. Fitzgerald, and W. R. Tribe, Proc. SPIE **5070**, 44 (2003).

⁹F. Oliveira, R. Barat, B. Schulkin, J. Federici, D. Gary, and D. Zimdars, Proc. SPIE **5070**, 60 (2003).

¹⁰R. Appleby, Proc. SPIE **5077**, 1 (2003); A. H. Lettington, D. Dunn, I. M. Blankson, and M. F. Attia, *ibid.* **5077**, 22 (2003).

¹¹N. A. Salmon, Proc. SPIE **5077**, 71 (2003).